Cross sign T2 hyperintensities in atrophic spinal cord of hereditary spastic paraplegia type 5

Ning Wang
First Affiliated Hospital of Fujian Medical University
Ying Liu
First Affiliated Hospital of Fujian Medical University
Zhixian Ye
Fujian Medical University
Yi Lin
First Affiliated Hospital of Fujian Medical University
Xiang Lin
First Affiliated Hospital of Fujian Medical University
Yi-Jun Chen
Fujian Medical University
Meng-Wen Wang
Fujian Medical University
Jianping Hu
First Affiliated Hospital of Fujian Medical University
Wenjie Cai
Fujian Medical University
Qiang Weng
Fujian Medical University
Yi-Heng Zeng
Fujian Medical University
Gui-He Li
Fujian Medical University
Xue-Jing Huang
Fujian Medical University
Yaou Liu
Capital Medical University
Wan-Jin Chen
First Affiliated Hospital of Fujian Medical University
Dairong Cao
First Affiliated Hospital of Fujian Medical University
Ying Fu (fuying@fjmu.edu.cn)

Fujian Medical University https://orcid.org/0000-0002-1590-3945

Research article

Keywords: Hereditary spastic paraplegias type 5, Neuroimaging features, Diagnostic biomarkers, Quantitative volumetry, Pathological features

Posted Date: October 30th, 2020

DOI: https://doi.org/10.21203/rs.3.rs-97876/v1

Abstract

Background: Hereditary spastic paraplegias type 5 (SPG5) is an inherited neurodegenerative disease with 27-hydroxycholesterol abnormal accumulation. Imaging and pathologic manifestations remain poorly understood due to the rare incidence. This study reveals the MRI features of SPG5, and aims to investigate a promising imaging diagnostic biomarker for SPG5.

Methods: We prospectively recruited SPG5 patients and matched healthy controls from Neurogenetic Diseases Centers of Fujian province in China, clinical and MRI data of whom were collected. Abnormalities of spinal cord and brain were characterized and quantified by conventional and quantitative MRI. Comparisons were conducted between MRI and cerebrospinal fluid (CSF) bioindicators.

Results: Seventeen SPG5 patients were enrolled (11 men, 6 women; age range, 13–49 years; median disease duration, 14 years). For the first time, T2 hyperintensities with "+" form (cross sign) in atrophic spinal cord was found among all SPG5 patients. To grade severity of this sign, we set up a scoring scale (cross-sign scores) in cervical spinal cords. Unexpectedly, total cross-sign scores showed a strong positive correlation with disability scale scores ($r = 0.687$, $P = 0.002$) and disease duration ($r = 0.520$, $P = 0.032$). Although total spinal cord area was reduced (cervical levels: 12-27%; thoracic levels 41-60%), no correlation was found between spinal cord atrophy and disease severity. In CSF, a positive correlation was identified between 27-hydroxycholesterol and neurofilament light ($r = 0.468$, $P = 0.049$), although 27-hydroxycholesterol and neurofilament light were unrelated to disease severity.

Conclusion: Cross sign of spinal cord was established as a potentially diagnostic biomarker linked to SPG5 that can guide genetic testing and interpret genetic results. Moreover, cross-sign scoring scale is more sensitive than spinal cord area and CSF markers for monitoring SPG5 progress in our research.

Background

Hereditary spastic paraplegias (HSP) are a large, genetically diverse group of inherited neurological disorders characterized by a length-dependent distal axonopathy of the corticospinal tract, resulting in lower limb spasticity and weakness(1). Hereditary spastic paraplegia type 5 (SPG5), a subtype of HSP, is caused by autosomal recessive loss-of-function mutations in *CYP7B1*, that encodes oxysterol-7a-hydroxylase. This mutations leads to the accumulation of *CYP7B1* substrates, such as 27-hydroxycholesterol (27-OHC), in plasma and CSF(2, 3).

Previous reports have indicated that hypercholesterolemia confers a higher risk for Alzheimer's disease, and evidences suggest that 27-OHC plays a pivotal role in Alzheimer's-associated neural injury (4–6). As an oxidized derivative of cholesterol, 27-OHC has cytotoxic and pro-apoptotic properties, which is increased approximately 0.5-fold (40–80 ng/mL) in patients with cognitive impairment and 10-fold (600–1300 ng/mL) in patients with SPG5 (3, 7). The observation of extremely high levels of 27-OHC prompted us to hypothesize that an accumulation of neurotoxic oxysterols could cause abnormalities in the spinal cord and brain. In fact, T2 white matter hyperintensities of the brain have been reported in case studies of

SPG5(8),[9]. However, image manifestations of SPG5 are poorly understood owing to limited diagnostic tools for many patients.

Our center focuses on HSP research and have set up an HSP cohort to record natural disease history. To date, 34 SPG5 patients have been long-term followed, 28 of whom were previously reported(10). In this study, we applied conventional and quantitative MRI techniques to characterize and quantify signal and structural changes of spinal cord and brain among SPG5 patients. Subsequently, we analyzed the correlations between MRI-derived measurements with the clinical status and molecular biomarkers of these patients.

Methods

Standard protocol approvals, registrations, and patient consents

The study protocol and informed consent procedures were approved by the institutional review board at First Affiliated Hospital of Fujian Medical University. This study is registered with ClinicalTrials.gov, number: NCT04006418.

Participants

We enrolled SPG5 patients from an HSP cohort at the Neurogenetic Diseases Centers in the First Affiliated Hospital of Fujian Medical University in Fuzhou, China for comparison with age- and sex-matched healthy controls. SPG5 patients with clinically manifested HSP and genetic confirmation were eligible to participate in this study. Exclusion criteria were patients with (1) other neurologic or systemic diseases, (2) substance abusers, (3) other causes of focal or diffuse brain and spinal cord damage determined by routine MRI sessions, (4) restrictions for MRI scanning, and (5) restrictions for lumbar puncture. Of the 34 patients considered for this trial, 17 met all of the specified criteria. Clinical and MRI data were then collected August 31, 2019 and November 17, 2019.

Healthy controls underwent neurologic evaluation and MRI examination, and were included only if they had normal findings.

Clinical and biochemical assessments

Clinical data, CSF, and blood were collected for analyses according to standard protocols. On the day of MRI scans, each patient had a full neurological evaluation by an experienced neurologist. The disease severity was quantified using the Spastic Paraplegia Rating Scale (SPRS). After overnight fasting (12 hours), patients underwent blood collection by venipuncture at room temperature. Simultaneously, CSF was also collected via lumbar puncture, and all samples were stored at -80 °C until use. CSF 27-OHC was analyzed by ultra-performance liquid chromatography-tandem mass spectrometry (UPLC-MS/MS) and quantified with a stable isotope dilution method. CSF neurofilament light (NFL) was detected using the Simoa NF-Light Advantage Kit (Quanterix) on a Simoa HD-1 Analyzer instrument, according to the manufacturer's instructions.

MRI data acquisition

All subjects were examined with a 3T Siemens scanner (MAGNETOM Skyra) equipped with a 20-channel head-neck coil and a 24-channel spine-array coil. Cervical and thoracic spinal cord images were obtained by 3D T2-weighted turbo spin-echo sequence (Sampling Perfection with Application-optimized Contrast using different flip angle Evolutions, SPACE), 3D-T1-weighted turbo spin-echo sequence (magnetization prepared rapid acquisition gradient echo, MPRAGE) in the sagittal plane, and three axial conventional sequences [2D T2* (Multiple Echo Date Image Combination, MEDIC), 2D T2-PD, 2D T2]. Brain images were obtained by 3D T1- MPRAGE in the sagittal plane and T2, FLAIR, and SWI in the axial plane. The parameters of the main MRI sequences are listed in **Table e-1**.

Image analyses

Specific radiological sign assessment in spinal cord

This report provides the first description of a T2 hyperintensity cross sign in the spinal cords of SPG5 patients, a form of hyperintensity resembling a "+" observed in T2* MEDIC, T2-PD, and T2 sequences. This sign corresponds with the symmetric hyperintensities of the anterior and dorsal columns with a preserved anterior horn (in contrast with a blurred dorsal horn) on the T2* MEDIC sequence (Fig. 1).

Cross-sign scoring (CSS) scale was performed according to the following observations (outlined in Fig. 2): 0, normal signal morphology of the spinal cord; 1, hyperintense signal of the anterior and dorsal columns; 2, hyperintense signal of the anterior and dorsal columns and blurred signals on the dorsal horn; 3, hyperintense signal of the anterior and dorsal columns and lost signals of the dorsal horn. The thoracic T2*-MEDIC datasets of all patients and healthy controls were excluded due to technical limitations, so cross sign was assessed only in the C2 to C7 vertebral disc levels. A single axial T2*-MEDIC image of the most affected slice in every intervertebral disc level was identified for scoring. The two participating radiologists were instructed in the rating system for this study (C.D.R. who has 30 years of neuroradiology experience and Y.L. who has 10 years of neuroradiology experience); both were blinded to the clinical information. The intraclass correlation coefficients were also calculated. The summed scores of all intervertebral disc levels were recorded.

Spinal cord cross-sectional area measurement

After completion of the MRI scans, the 3D T2 images of the cervical and thoracic spine areas were simultaneously stitched to ensure full presentation of each cervicothoracic spinal cord (C1-T9) acquired by Compose software on a SIEMENS workstation (Fig. 3A). Spinal cord segmentation and cross-sectional area measurements were performed using Spinal Cord Toolbox, Version 4.01 (https://sourceforge.net/projects/spinalcordtoolbox/). Morphological spinal cord metrics were extracted at each vertebral level (from C1 to T9), including spinal cord cross-sectional area and sectional diameter, for further analyses.

Conventional brain MRI evaluation

Abnormal signals were assessed in T2, T1, FLAIR, and SWI routine sequences. Some neuroradiological signs, which have been previously reported in specific subtypes of HSP(11), were also analyzed in the current SPG5 patients.

Visual rating of cerebral atrophy
Visual rating of 3D T1 images from each participant was performed by two experienced neurologists who were trained for consistency in scale evaluation. Images were rated in native space with RadiAnt DICOM Viewer software. Six regions were rated based on existing scales and a simplified version of the overall rating was used with a detailed evaluation protocol, as previously described(12).

Quantitative brain MRI evaluation

Voxel-based morphometry (VBM) was performed to assess alterations in brain volume and grey matter volume (GMV) of patients with SPG5 compared to healthy controls. The GMV of each subject was processed using the CAT12 toolbox (http://dbm.neuro.uni-jena.de/cat/), incorporated in SPM12 (www.fil.ion.ucl.ac.uk/spm), running under MATLAB R2016a. Corpus callosum volumes were calculated using a script file written by Ged Ridgway (http://www0.cs.ucl.ac.uk/staff/g.ridgway/vbm/get_totals.m), also running under MATLAB R2016a. Cerebellum volume was manually measured with MRIconN (https://www.nitrc.org/projects/mricron).

Statistical analyses

Results are expressed as median with range for continuous variables and probability for categorical variables. Kolmogorov-Smirnov tests were used to assess the normality of the variables. For normally distributed variables, differences were assessed using Student's *t*-test, and associations were assessed by Pearson correlation analyses. For variables that were not normally distributed or non-parametric, differences were assessed using the Mann-Whitney test, and associations were assessed with the Spearman correlation analyses. Categorical variables were compared for the groups using the *Chi*-squared test (Fisher's exact test when the expected value is < 5).

Statistical analyses of structural image data were conducted as follows: voxel-based independent two sample t-test was performed to analyze differences in GMV between healthy controls and SPG5 patients. Statistical tests were evaluated at a significance level of $P < 0.05$, corrected for multiple comparisons, with the false discovery rate (FDR) at the voxel level. Analyses were processed with SPSS software (version 25; IBM, USA).

Results

Characteristics of SPG5 patients

Seventeen SPG5 patients, including five with consanguinity, were consecutively enrolled from 14 families. Sixteen patients from 13 unrelated families carried the known nonsense homozygous mutation c.334 C > T (p.R112*). Only one patient carried compound heterozygous mutations c.259 + 2T > C and c.1190C > T (**Table e-2**).

Age at onset ranged from 1 to 27 years with a median of 11 years. Patients had a median duration of 14 years (range 6–40). All patients exhibited a moderate spastic paraplegia with a median SPRS score of 15 (range 2–38). According to Harding criteria based on clinical phenotype, 16 patients were classified as pure HSP and one was complicated HSP with epilepsy. Sixteen patients had severely reduced or nonexistent vibration sense in the lower limbs, and one patient had urinary urgency. None had cognition injury, cerebellar ataxia or axonal peripheral neuropathy (**Table e-2**).

Healthy controls matched SPG5 patients in terms of age [median (range), 30 (13–49) vs 30 (14–50), P = 1.000] and gender (male %, 65% vs 65%, P = 1.000).

Biochemical assessments

The median concentration of CSF 27-OHC was 10 ng/ml (range 7–13), and the median concentration of CSF NFL was 531 pg/ml (range 290–764). Spearman coefficients demonstrated a positive correlation between CSF 27-OHC and CSF NFL (r = 0.468, P = 0.049). However, 27-OHC and NFL in the CSF exhibited no significant relationship with disease severity or duration.

Spinal cord cross sign assessment

Regardless of disease duration and severity, all SPG5 patients manifested spinal cord cross sign in three MRI sequences (T2*-MEDIC, T2-PD, T2). This sign manifested as a symmetric hyperintense signal of the anterior and dorsal columns with a preserved anterior horn (the dorsal horn appears blurred). In contrast, none of the healthy controls exhibited such a specific sign (Fig. 1).

Cross sign scoring was performed by two experienced radiologists using the observational criteria outlined in Fig. 2A-B. Inter-scorer reliability assessment of reliability between radiologist scorers showed intraclass correlation coefficients from 0.9 to 0.95 at all levels (P < 0.001), thus demonstrating high reproducibility between observers. Cross signs were more pronounced at the C2 and C7 levels among all the explored cervical segments (Fig. 2A): C2, 3 (2–3); C3, 2 (1–3); C4, 2 (1–3); C5, 1 (1–3); C6, 2 (1–3); C7, 2 (2–3).

Total cross sign scores correlated with the disease severity. Spearman coefficients demonstrated positive correlations between total cross sign scores and SPRS (r = 0.687, P = 0.002) as well as disease duration (r = 0.520, P = 0.032). However, total cross sign scores did not correlate with either CSF 27-OHC or CSF NFL concentrations.

Spinal cord atrophy quantification

Since the proposed processing pipeline was fully automated, automatic registration into the Spinal Cord Toolbox template was successful in most cases (Fig. 3A). Manual correction was needed for the spinal cord segmentation of only 2 subjects (1 patient and 1 healthy control).

Spinal cord areas were significantly smaller in patients than in controls at all the evaluated cervical and thoracic levels (Fig. 3B-D). Moreover, the relative reduction in area was more pronounced at the thoracic levels (cervical levels: 12–27%; thoracic levels 41–60%), especially in T4 (35 vs 22 mm^2, P < 0.001). At the

T4 level, the relative reduction of antero-posterior diameters was greater than the reduction in transverse diameters (24% vs 18%, P = 0.101). The area under the ROC for the T4 spinal cord area was 0.976 (P < 0.001), and the cut-off value was 29 mm^2 (sensitivity 88% and specificity 94%).

In no instance did the total spinal cord area or spinal cord area at any of the examined levels correlate with disease duration, clinical scores, CSF 27-OHC, or CSF NFL (P > 0.05).

Conventional MRI findings in the brain

No signal abnormalities were observed in the brain T2, FLAIR, or SWI sequences of any SPG5 patients or healthy controls. None of the specific signs that have been previously reported for subtypes of HSP appeared in any of these SPG5 patients, including “Ear-of-the-lynx” sign, enlarged ventricles, brain white matter T2 hyperintensities, and bilateral T2 hypo-signal of the globus pallidus (Fig. 4).

Brain atrophy measurements

Based on MRI visual rating scales, there were no differences in cerebral atrophy assessed with scores for each region or total scores from SPG5 patients compared to healthy controls (Fig. 5A).

Based on voxels measurement, compared to healthy controls, there were no significant differences in total intracranial volume (TIV, 1517 vs 1564 ml, P = 0.652), grey matter volume (GMV, 666 vs 699 ml, P = 0.179), white matter volume (WMV, 539 vs 536 ml, P = 0.926) or CSF volume (308 vs 287 ml, P = 0.152) (Fig. 5B). Grey matter fraction (GMF) was calculated using the formula: GMF = GMV/TIV, where TIV = GMV + WMV + CSF volume. Significantly lower GMF was observed in SPG5 patients (0.43 vs 0.45, P = 0.03) (Fig. 5C). The GMV was then applied to normalize the raw volumes of brain structures. The normalized GMV of the bilateral thalamus in SPG5 differed from those of healthy controls (peak t value = 6.77, P < 0.05, FDR corrected at voxel-level) (Fig. 5D). No significant differences from controls were found in cerebellum volume [135 (95–161) vs 132 (114–163) mL, P = 0.563] or corpus callosum volume [37 (34–38) vs 37 (35–38) mL, P = 0.779), or their volume fractions (Fig. 5E-F).

Discussion

Since the core clinical imaging features of SPG5 has not been described previously, we undertook the present study not only to provide a detailed characterization of the structural signature of SPG5, but also to investigate what specific patterns of spinal cord and brain damage correlate with clinical and pathogenic manifestations. To accomplish these goals, we enrolled a relatively large set of patients who underwent systematic clinical assessment combined with multimodal MRI and CSF markers evaluations. As a result, we have described the neuroimaging findings from both clinical and molecular pathologic viewpoints. First, the signal abnormality at cervical levels was reliably reflected by conventional spinal cord MRI among the SPG5 patients, and “+” T2 hyperintensities (cross sign) in the atrophy spinal cord appeared in all 17 patients. Second, we set up cross sign scoring to grade the severity of this sign, and subsequently found that total cross sign scores bore a strongly positive correlation with the extent of disease degeneration, as assessed by standardized disability scales and disease duration. Third, as

expected, each total spinal cord area had decreased significantly at each site investigated, in comparison with those of healthy controls, especially in the T4 level. However, no correlation was evident between spinal cord area and either disability or pathogenesis-associated molecular biomarkers. Fourth, no abnormality was present in conventional brain MRI or quantitative brain MRI-derived data, with the exception of a mildly reduced gray matter on the thalami.

T2 hyperintensities in spinal cord MRI are commonly associated with a large variety of causes (inflammation, infections, neoplasms, vascular, and spondylotic diseases), but it is rarely caused by HSP, except as reported for hereditary spastic paraplegias type 2 (SPG2), due to *PLP1* gene mutations(13).

In this study, the included SPG5 patients were retained for long-term follow-up and, no other disease was identified. The cross sign spinal cord T2 hyperintensities, first defined in this report, appeared in all 17 of our patients on three different sequences (T2, T2-PD, T2*-MEDIC), and differed from the T2 hyperintensity morphology in patients with SPG2. Thus, this spinal cord cross sign is a specific imaging feature for SPG5 and can therefore serve as a potentially useful diagnostic biomarker for SPG5, both in guidance for genetic testing or as a reference for interpreting genetic findings.

Upon further investigation, we found that the spinal cord of SPG5 patients was atrophied but without correlation to the extent of disability or duration of disease, as reported for other subtypes of HSP(14). The lack of correlation may be partially explained by slow progression of SPG5 and low sensitivity of the imaging biomarker (spinal cord area). In contrast, the total cross sign score may provide a more sensitive imaging marker than other features of the spinal cord for quantifying the degree of neurodegeneration. As such, the cross-sign scores can be a valuable and informative imaging biomarker for monitoring disease process as well as the therapeutic response of SPG5 patients.

The accumulation of 27-OHC may be not only a biomarker but also a key factor in driving tissue damage in patients with SPG5. NFL is a protein component of the cytoskeleton of myelinated axons, and, as such, constitutes a putative biomarker to reflect axonal injury(15–17). Further, the concentration of CSF 27-OHC, which had a positive correlation with CSF NFL concentration in our study, could potentially indicate an association of neurotoxic 27-OHC with axonal injury. However, no significant correlation was identified between the concentrations of 27-OHC or NFL in the CSF with the progressive degeneration shown in clinical load (SPRS, disease duration) or in the worsening imaging indicators (total cross sign scores, spinal cord area). Therefore, although CSF 27-OHC and CSF NFL may be suitable markers for monitoring disease activities, they are not useful guides to the overall progression of SPG5.

Surprisingly, we failed to identify obvious cerebral atrophy in SPG5 through two advanced imaging techniques (visual rating of cerebral atrophy and quantitative brain measurements), as reported in Alzheimer's disease(18). However, emerging evidence has revealed common pathological mechanisms in neuronal injury from 27-OHC in familial Alzheimer's disease and SPG5(6, 19–21). In contrast, spinal cord morphometry indicated more substantial atrophy in SPG5 patients. Moreover, specific T2 hyperintensities visible on spinal cord MRI support the likelihood that severe spinal cord damage from 27-OHC might be implicated in SPG5 pathogenesis.

SPG5 (*CYP7B1* gene mutation) and cerebrotendinous xanthomatosis (CTX, *CYP27A1* gene mutation) are neurological diseases with mutations in genes that participate in cholesterol metabolism (22–24). Rare cases of genetically and biochemically confirmed 'spinal CTX' have been reported(25–30). Spinal CTX differs from the classical cases with a relatively benign course, whose clinical presentations are dominated by spinal symptoms (spastic paraplegia, alteration to deep sensation, and urinary involvement), and paucity or absence of the classical neurological and systemic symptoms. These clinical features are almost indistinguishable from SPG5. In spinal CTX patients, spinal MRI studies revealed longitudinally extensive posterior and lateral column white matter abnormalities on T2 images, which strongly resemble our observations in SPG5 patients(29),(30). Together, the mutations associated with cholesterol metabolism and similar clinical and spinal cord MRI features suggest the likelihood of a similar pathogenic mechanisms for spinal cerebrotendinous xanthomatosis and SPG5.

Conclusion

In this work, we provide the first evidence to our knowledge that T2-associated sequences show "+" signal hyperintensities in the atrophied spinal cords of SPG5 patients, and that this "cross sign" is associated with disease-related degeneration. This imaging sign can reinforce the validity of diagnoses, facilitate assessment of disease progression, and assist in monitoring of therapeutic effects. More importantly, the identification of new imaging features in SPG5 provides fresh insight into the pathogenic mechanism for oxidized derivatives of cholesterol.

Abbreviations

AC: Anterior cingulate; AT: Anterior temporal; CSF: Cerebrospinal fluid; CSS: Cross-sign scoring; CTX: Cerebrotendinous xanthomatosis; FDR: False discovery rate; FI: Fronto-insular cortex; GMF: Grey matter fraction; GMV: Grey matter volume; HC: Healthy control; HSP: Hereditary spastic paraplegias; MEDIC: Multiple Echo Date Image Combination; MPRAGE: Magnetization prepared rapid acquisition gradient echo; MT: Medial temporal lobe; NFL: Neurofilament light; OF: Orbitofrontal cortex; PA: Posterior cortex; SCA: Spinal cord cross-sectional area; SPG2: Hereditary spastic paraplegias type 2; SPG5: Hereditary spastic paraplegias type 5; SPM: Statistical Parametric Mapping; SPRS: Spastic Paraplegia Rating Scale; T-CSS: total cross sign scoring; TIV: Total intracranial volume; 27-OHC: 27-hydroxycholesterol; VBM: Voxel-based morphometry; WMV: White matter volume.

Declarations

Ethical approval and consent to participate

Informed written consents were obtained from all the participants. This study was approved by the Ethics Committee of the First Affiliated Hospital of Fujian Medical University (MRCTA,ECFAH of FMU [2019]209-1).

Consent for publication

Not applicable.

Competing interests

The authors declare that they have no competing interests.

Funding

This work has been supported by the grants 81771279 (YF) and 81801130 (XL) from the National Natural Science Foundation of China, Joint Funds for the Innovation of Science and Technology of Fujian Province (2017Y9094) (WJC) and (2018Y9082) (NW), the Natural Science Foundation of Fujian Province (2019J02010) (WJC) and (2019J05076) (XL), the Key Clinical Specialty Discipline Construction Program of Fujian (NW). All authors report no disclosures.

Authors' contributions

YF, NW, WJC. and CDR formulated the study concept and designed this trial; YL, YJC, MWW, YHZ, GHL and XJH enrolled the patients and conducted clinical assessments; YL, ZXY, JPH, WJC and QW conducted imaging scanning and data collection; XL, YJC and MWW performed laboratory determination; YF, ZXY, DRC, WJC and YL analyzed the data, interpreted the results and drafted the manuscript; YOL offered clinical and imaging expertise and contributed to preparation of the manuscript. All authors read and approved the final manuscript.

Acknowledgments

We sincerely thank our patients for participating in this study, Ms. P. Minick for editorial assistance.

References

1. Salinas S, Proukakis C, Crosby A, Warner TT. Hereditary spastic paraplegia: clinical features and pathogenetic mechanisms. Lancet Neurol. 2008;7(12):1127–38.
2. Shribman S, Reid E, Crosby AH, Houlden H, Warner TT. Hereditary spastic paraplegia: from diagnosis to emerging therapeutic approaches. Lancet Neurol. 2019;18(12):1136–46.
3. Schols L, Rattay TW, Martus P, Meisner C, Baets J, Fischer I, et al. Hereditary spastic paraplegia type 5: natural history, biomarkers and a randomized controlled trial. Brain. 2017;140(12):3112–27.
4. Ismail MA, Mateos L, Maioli S, Merino-Serrais P, Ali Z, Lodeiro M, et al. 27-Hydroxycholesterol impairs neuronal glucose uptake through an IRAP/GLUT4 system dysregulation. The Journal of experimental medicine. 2017;214(3):699–717.
5. Kivipelto M, Helkala EL, Laakso MP, Hanninen T, Hallikainen M, Alhainen K, et al. Midlife vascular risk factors and Alzheimer's disease in later life: longitudinal, population based study. Bmj.

2001;322(7300):1447–51.

6. Hottman DA, Chernick D, Cheng S, Wang Z, Li L.. . ; Pt. HDL and cognition in neurodegenerative disorders. Neurobiol Dis. 2014;72:A:22–36.
7. Liu Q, An Y, Yu H, Lu Y, Feng L, Wang C, et al. Relationship between oxysterols and mild cognitive impairment in the elderly: a case-control study. Lipids Health Dis. 2016;15(1):177.
8. Biancheri R, Ciccolella M, Rossi A, Tessa A, Cassandrini D, Minetti C, et al. White matter lesions in spastic paraplegia with mutations in SPG5/CYP7B1. Neuromuscul Disord. 2009;19(1):62–5.
9. Lan MY, Yeh TH, Chang YY, Kuo HC, Sun HS, Lai SC, et al. Clinical and genetic analysis of Taiwanese patients with hereditary spastic paraplegia type 5. Eur J Neurol. 2015;22(1):211–4.
10. Dong EL, Wang C, Wu S, Lu YQ, Lin XH, Su HZ, et al. Clinical spectrum and genetic landscape for hereditary spastic paraplegias in China. Mol Neurodegener. 2018;13(1):36.
11. da Graca FF, de Rezende TJR, Vasconcellos LFR, Pedroso JL, Barsottini OGP, Franca MC. Jr. Neuroimaging in Hereditary Spastic Paraplegias: Current Use and Future Perspectives. Front Neurol. 2018;9:1117.
12. Harper L, Fumagalli GG, Barkhof F, Scheltens P, O'Brien JT, Bouwman F, et al. MRI visual rating scales in the diagnosis of dementia: evaluation in 184 post-mortem confirmed cases. Brain. 2016;139(Pt 4):1211–25.
13. Marelli C, Salsano E, Politi LS, Labauge P. Spinal cord involvement in adult-onset metabolic and genetic diseases. J Neurol Neurosurg Psychiatry. 2019;90(2):211–8.
14. Faber I, Martinez ARM, de Rezende TJR, Martins CR Jr, Martins MP, Lourenco CM, et al. SPG11 mutations cause widespread white matter and basal ganglia abnormalities, but restricted cortical damage. Neuroimage Clin. 2018;19:848–57.
15. Khalil M, Teunissen CE, Otto M, Piehl F, Sormani MP, Gattringer T, et al. Neurofilaments as biomarkers in neurological disorders. Nat Rev Neurol. 2018;14(10):577–89.
16. Kuhle J, Kropshofer H, Haering DA, Kundu U, Meinert R, Barro C, et al. Blood neurofilament light chain as a biomarker of MS disease activity and treatment response. Neurology. 2019;92(10):e1007-e15.
17. QF L, JJ YDLY. X, Y M, YC D, et al. Neurofilament light chain is a promising serum biomarker in spinocerebellar ataxia type 3. Molecular neurodegeneration. 2019;14(1):39.
18. Ferreira D, Cavallin L, Larsson E, Muehlboeck J, Mecocci P, Vellas B, et al. Practical cut-offs for visual rating scales of medial temporal, frontal and posterior atrophy in Alzheimer's disease and mild cognitive impairment. Journal of internal medicine. 2015;278(3):277–90.
19. Björkhem I, Cedazo-Minguez A, Leoni V, Meaney S. Oxysterols and neurodegenerative diseases. Mol Aspects Med. 2009;30(3):171–9.
20. Testa G, Staurenghi E, Zerbinati C, Gargiulo S, Iuliano L, Giaccone G, et al. Changes in brain oxysterols at different stages of Alzheimer's disease: Their involvement in neuroinflammation. Redox Biol. 2016;10:24–33.

21. Brown J, Theisler C, Silberman S, Magnuson D, Gottardi-Littell N, Lee J, et al. Differential expression of cholesterol hydroxylases in Alzheimer's disease. J Biol Chem. 2004;279(33):34674–81.
22. Bjorkhem I, Leoni V, Meaney S. Genetic connections between neurological disorders and cholesterol metabolism. J Lipid Res. 2010;51(9):2489–503.
23. Theofilopoulos S, Griffiths WJ, Crick PJ, Yang S, Meljon A, Ogundare M, et al. Cholestenoic acids regulate motor neuron survival via liver X receptors. J Clin Invest. 2014;124(11):4829–42.
24. Kakiyama G, Marques D, Takei H, Nittono H, Erickson S, Fuchs M, et al. Mitochondrial oxysterol biosynthetic pathway gives evidence for CYP7B1 as controller of regulatory oxysterols. J Steroid Biochem Mol Biol. 2019;189:36–47.
25. Pilo-de-la-Fuente B, Jimenez-Escrig A, Lorenzo JR, Pardo J, Arias M, Ares-Luque A, et al. Cerebrotendinous xanthomatosis in Spain: clinical, prognostic, and genetic survey. Eur J Neurol. 2011;18(10):1203–11.
26. Bartholdi D, Zumsteg D, Verrips A, Wevers RA, Sistermans E, Hess K, et al. Spinal phenotype of cerebrotendinous xanthomatosis–a pitfall in the diagnosis of multiple sclerosis. J Neurol. 2004;251(1):105–7.
27. Mutlu D, Tuncer A, Gocmen R, Yalcin-Cakmakli G, Saygi S, Elibol B. Diagnostic challenge: A case of late-onset spinal form cerebrotendinous xanthomatosis. Neurology. 2019;92(9):438–9.
28. Gelzo M, Di Taranto MD, Bisecco A, D'Amico A, Capuano R, Giacobbe C, et al. A case of Cerebrotendinous Xanthomatosis with spinal cord involvement and without tendon xanthomas: identification of a new mutation of the CYP27A1 gene. Acta Neurol Belg. 2019.
29. Yanagihashi M, Kano O, Terashima T, Kawase Y, Hanashiro S, Sawada M, et al. Late-onset spinal form xanthomatosis without brain lesion: a case report. BMC Neurol. 2016;16:21.
30. Verrips A, Nijeholt GJ, Barkhof F, Van Engelen BG, Wesseling P, Luyten JA, et al. Spinal xanthomatosis: a variant of cerebrotendinous xanthomatosis. Brain. 1999;122(Pt 8):1589–95.

Figures

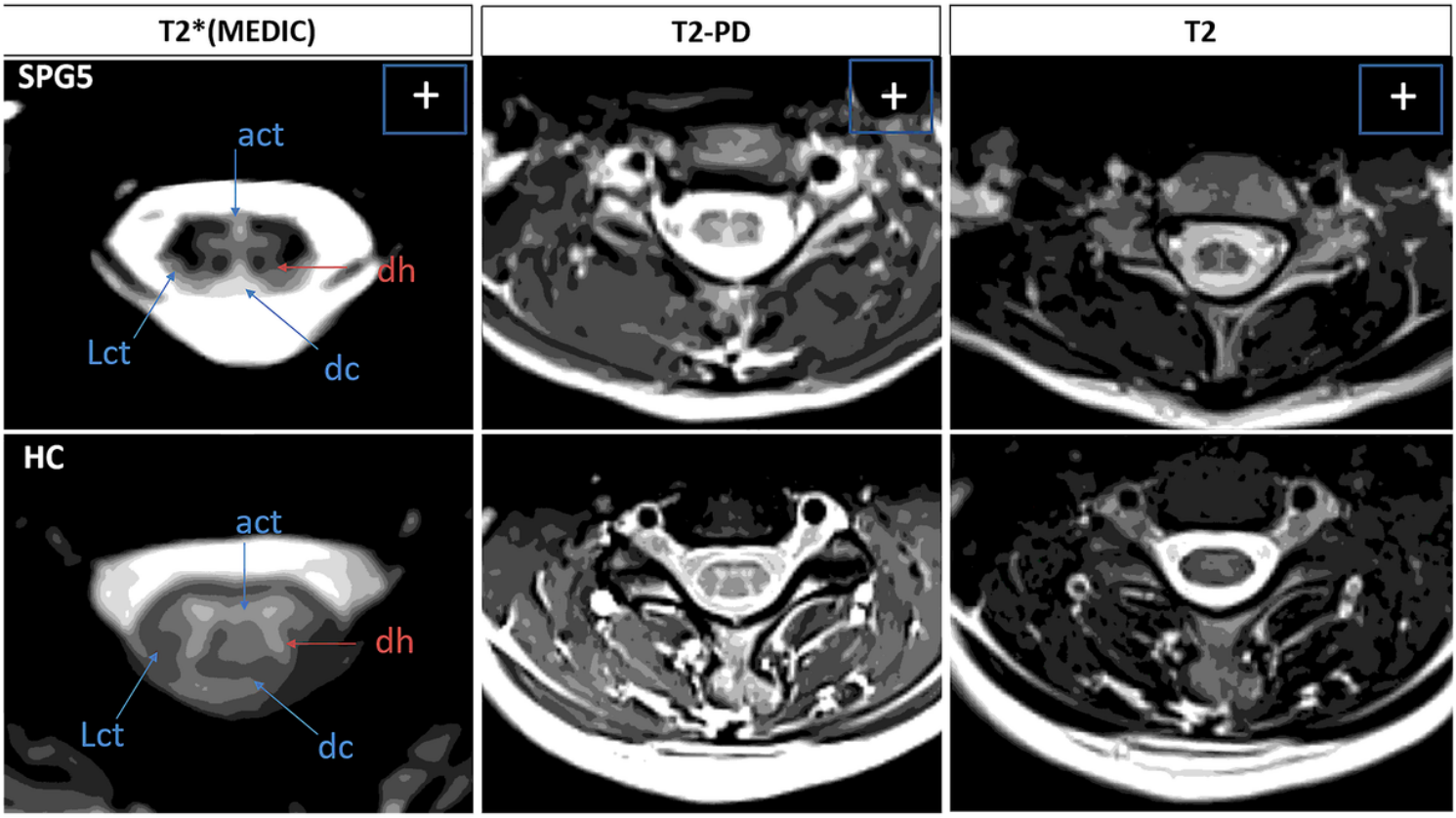

Figure 1

Cross sign appears on spinal cord MRI of the SPG5 patients Axial T2*MEDIC, T2-PD, and T2 images through cervical spinal cord: Above, an SPG5 female patient at the age of 18 years with 8 years disease duration and mild clinical signs (SPRS = 14); Below, a matched healthy control (female, 18 years old). The axial images at the level of the cervical spinal cord demonstrate that T2 hypersignals are confined to the dorsal columns (dc) and anterior(act) and lateral corticospinal tracts (lct); T2 signals of the dorsal horn (dh) have decreased or disappeared, and resemble a “+” in the center of the spinal cord, which we thus define as a “cross sign.”

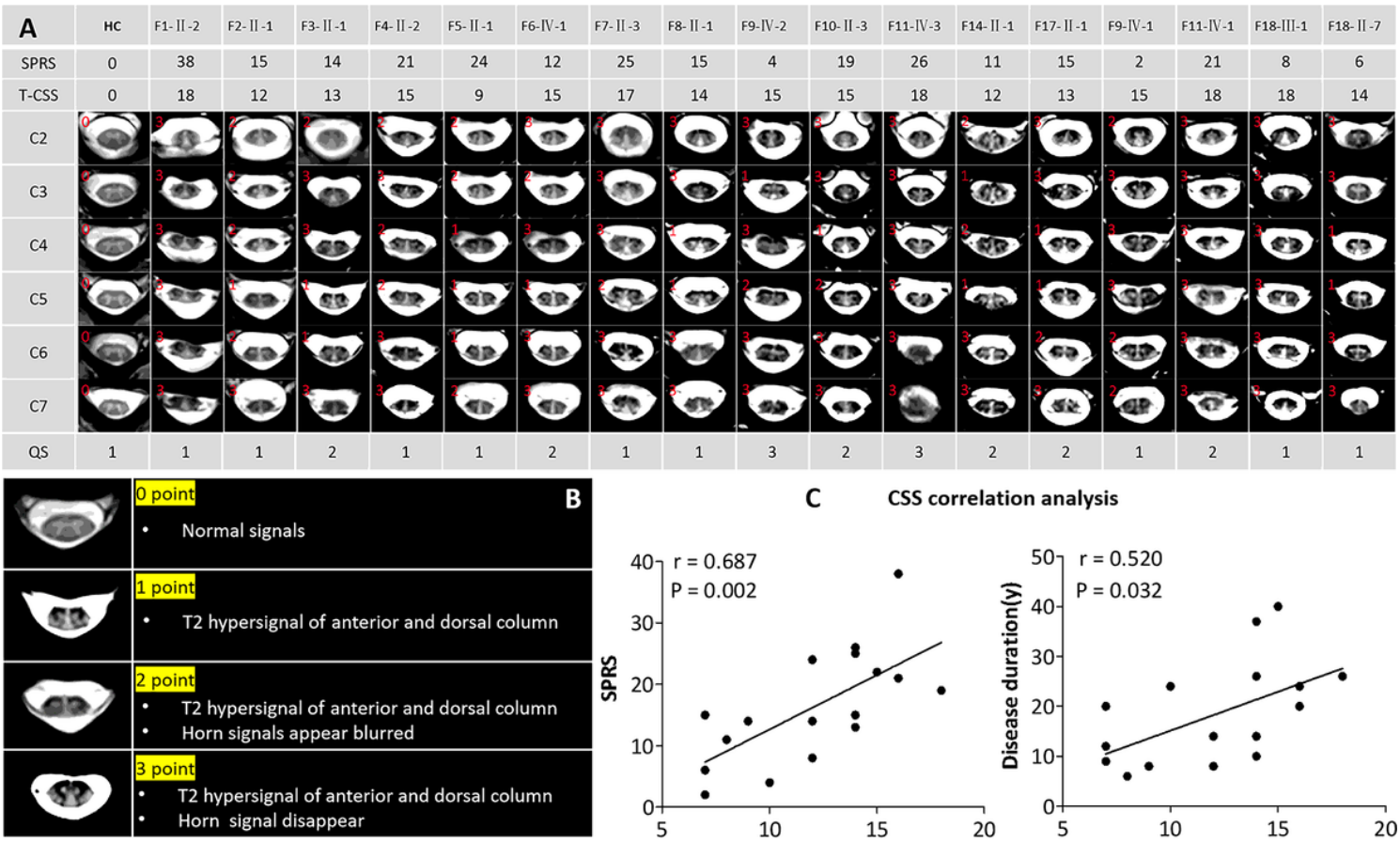

Figure 2

Individual and group analysis of cross sign scoring on T2* MEDIC imaging A: Axial cervical spinal cord (C2-C7) were obtained using 2D T2-weighted gradient echo sequence (Multiple Echo Date Image Combination, MEDIC), which provides strong contrast between white and grey matter; first column is a healthy control, others are SPG5 patients; all of the 17 SPG5 patients show the cross sign, but no healthy control has this radiological sign. QS = quality score, two radiologists visually assessed the quality of all the images and assigned a consensus score (1, good; 2, average; 3, bad). B: Cross sign scoring was set up to reflect the severity of the cross sign. C: Correlation analysis between SPRS scores and disease duration with total cross sign scoring (T-CSS), performed using the Spearman test. SPRS = Spastic Paraplegia Rating Scale, which reflects severity of the disease with higher scores indicating greater severity.

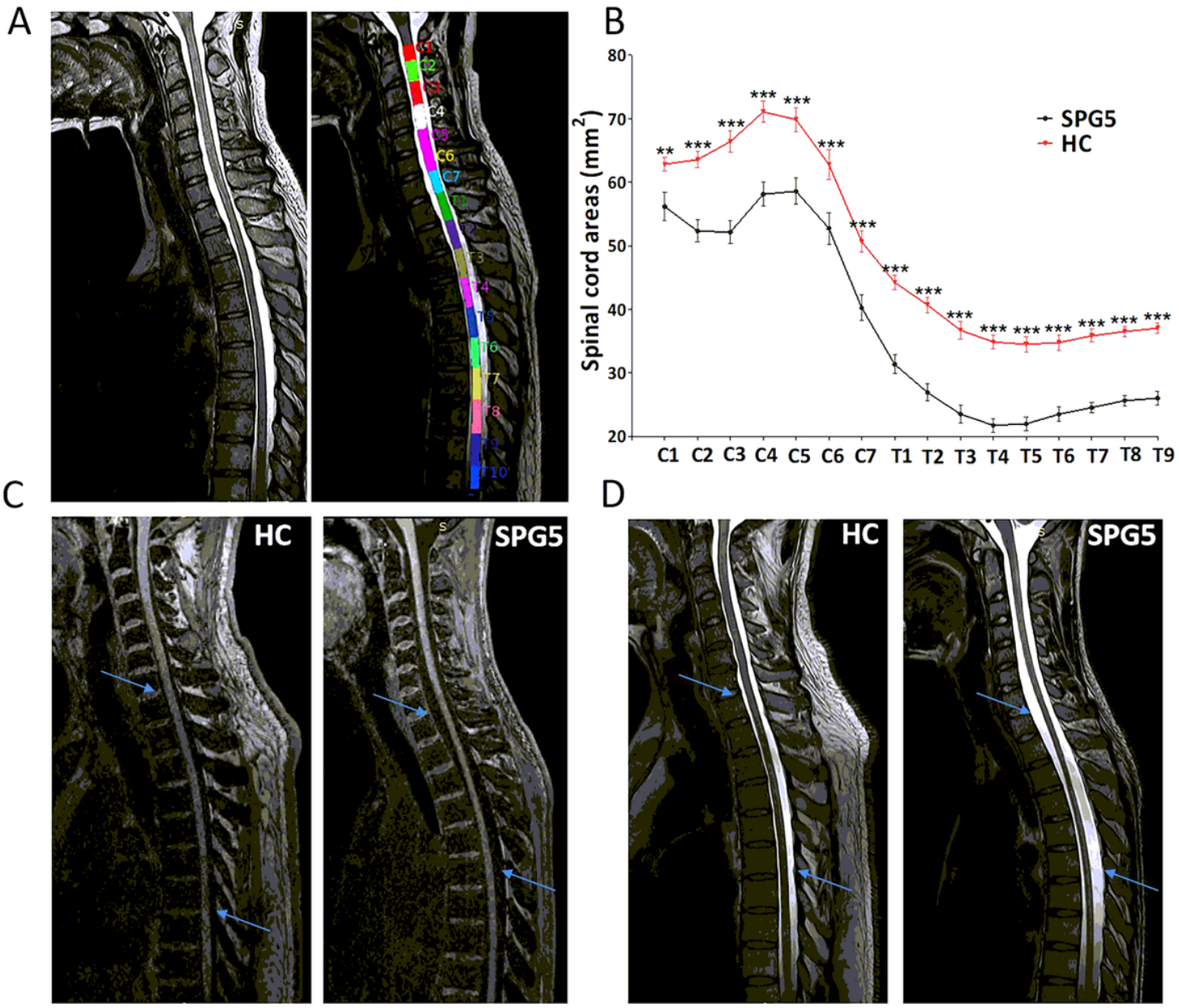

Figure 3

Quantitative MRI to assess spinal cord area A: Processing included three steps: 1) stitching together the composite cervical and thoracic spinal cord image with 3D-T2W-SPACE; 2) segmentation and labeling of the spinal cord; 3) measurement of spinal cord cross-sectional area (SCA) and sectional diameters (RL and AP). B: Comparisons of spinal cord areas (C2-T9) between SPG5 patients and matched healthy controls, performed using the Mann-Whitney test, **P <0.01, ***P <0.001. C-D: Representative MRIs of SPG5 and healthy controls. In SPG5 patients, a significant atrophy of the spinal cord was observed (blue arrow).

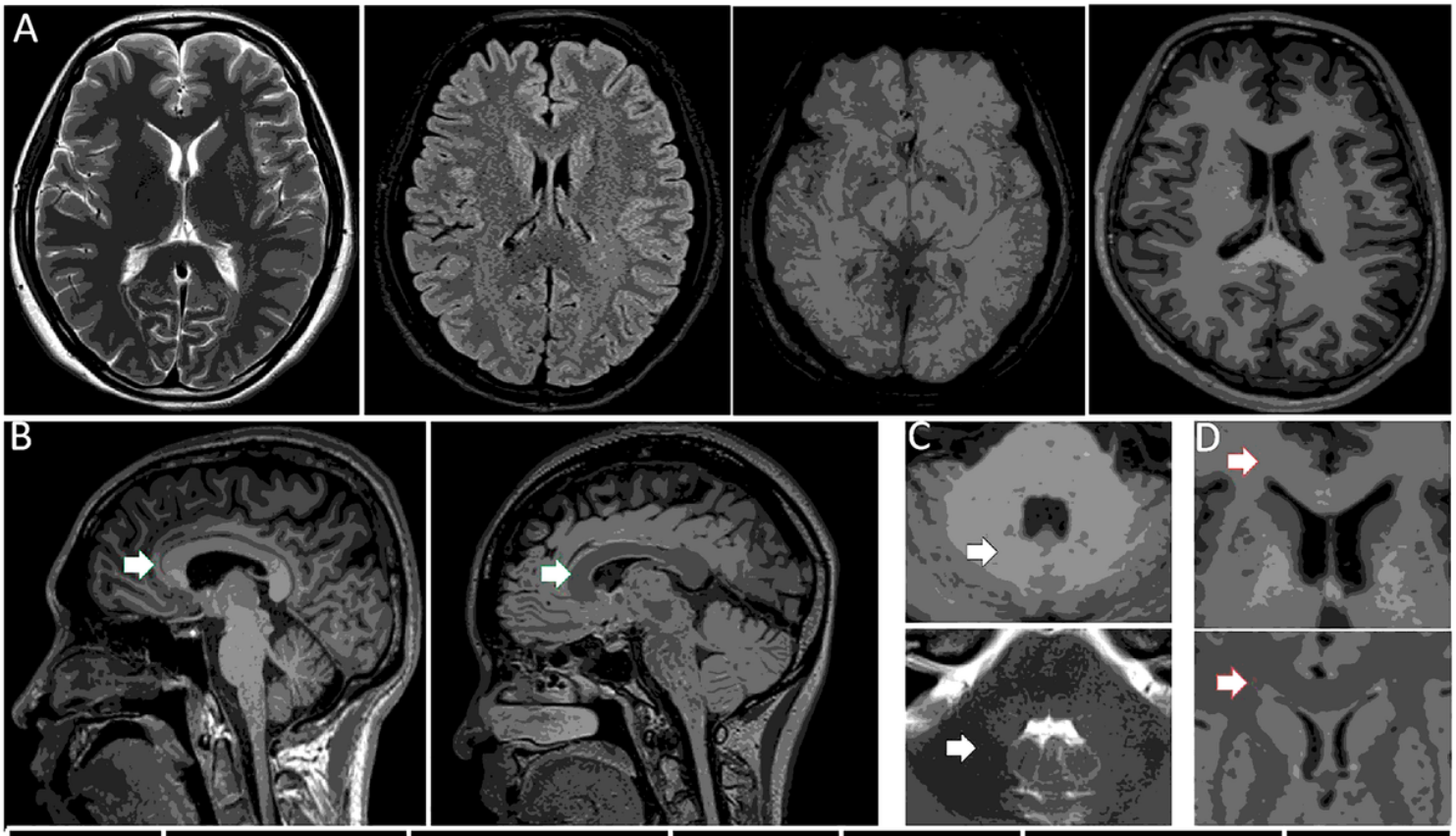

	White matter T2 hyperintensities	T2 hyposignal of globus pallidus	Enlarged ventricles	Thin corpus callosum	T2 hyperintensity of dentate nucleus	Ear-of-the-lynx sign
Positive	0	0	0	0	0	0
Negative	17	17	17	17	17	17

Figure 4

Conventional brain MRI evaluation A: Abnormal signals were assessed on T2, FLAIR, SWI, and T1 routine sequences (above panel, from left to right). B-D: Some neuroradiological signs, which have been reported in other subtypes of hereditary spastic paraplegias, were also assessed in these SPG5 patients ; B, atrophied corpus callosum (left T1, right T2, green arrow); C, T2 sequence hyperintensities of the dentate nucleus (Above T1, Below T2; black arrow); D, “Ear-of-the-Lynx” MRI sign (Above T1, Below T2, red arrow).

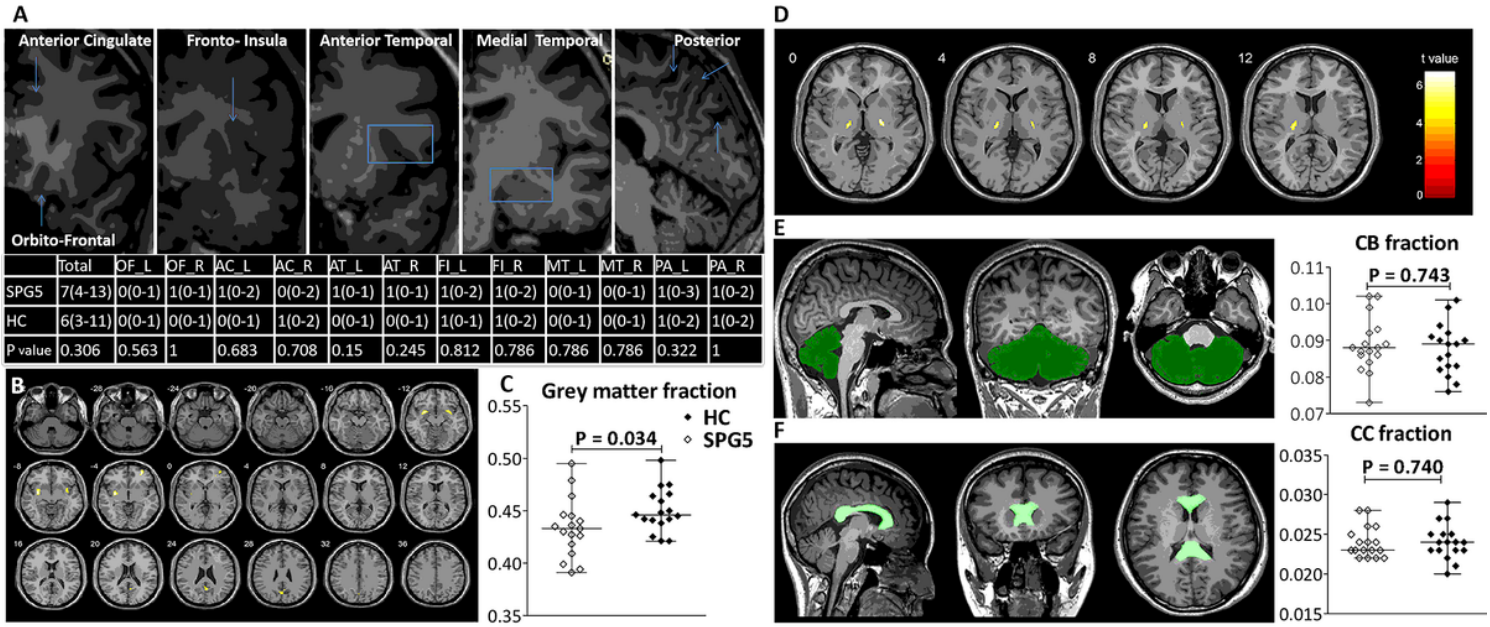

	Total	OF_L	OF_R	AC_L	AC_R	AT_L	AT_R	FI_L	FI_R	MT_L	MT_R	PA_L	PA_R
SPG5	7(4-13)	0(0-1)	1(0-1)	1(0-2)	0(0-2)	1(0-1)	1(0-1)	1(0-2)	1(0-2)	0(0-1)	0(0-1)	1(0-3)	1(0-2)
HC	6(3-11)	0(0-1)	0(0-1)	0(0-1)	1(0-2)	0(0-1)	0(0-1)	1(0-1)	1(0-2)	0(0-1)	0(0-1)	1(0-2)	1(0-2)
P value	0.306	0.563	1	0.683	0.708	0.15	0.245	0.812	0.786	0.786	0.786	0.322	1

Figure 5

Quantitative MRI to assess changes in brain structures A: Visual rating scales to assess cerebral atrophy, OF = orbitofrontal cortex, AC = anterior cingulate, AT= anterior temporal, FI = fronto-insular cortex, MT = medial temporal lobe, PA = posterior cortex; Comparisons of each visual rating score and total visual rating score between the SPG5 patients and the matched healthy controls (HC) were performed using the Mann-Whitney test. B: Voxel-based morphometry (VBM) was performed to assess alterations in brain volume between healthy controls (HC) and patients; statistical tests were evaluated at a significance level of $P < 0.05$, corrected by false discovery rate (FDR). C: Comparison of the grey matter fraction (GMF) between SPG5 patients and HC was performed using the Mann-Whitney test (right). D: VBM analysis was performed to assess differences in gray matter between HC and patients; statistical tests were evaluated at a significance level of $P < 0.05$ with FDR correction. E-F: Comparisons of the cerebellum volume fraction and corpus collosum volume fraction between SPG5 patients and HC were performed using the Mann-Whitney test.

Supplementary Files

This is a list of supplementary files associated with this preprint. Click to download.

- Additionalfile1.pdf
- Additionalfile2.pdf